Chemical and Topological Short Range Order of Amorphous Ti-Si Alloys

A. Pojtinger, R. Bellissent*, P. Lamparter, and S. Steeb
Max-Planck-Institut für Metallforschung, Seestrasse 92, D-70174 Stuttgart

Z. Naturforsch. **50a**, 749–757 (1995); received March 11, 1995

Amorphous $Ti_{100-x}Si_x$ alloys ($13 \leq x \leq 60$) were produced by sputtering. Their partial structure factors were determined by X-ray and neutron diffraction. The Bhatia-Thornton density-concentration correlation function $G_{NC}(R)$ was calculated by a cluster relaxation model. Three-dimensional atomic clusters were produced by the Reverse Monte Carlo method. These clusters were analyzed in terms of trigonal prismatic arrangements as a structural unit. In amorphous $Ti_{75}Si_{25}$ and $Ti_{87}Si_{13}$ those Si-atoms which are surrounded by 9 Ti-atoms in the first coordination shell prefer trigonal prismatic arrangements. In the atomic clusters of amorphous $Ti_{59}Si_{41}$, $Ti_{49}Si_{51}$, and $Ti_{40}Si_{60}$, however, no preference of trigonal prisms was found.

1. Introduction

The structure of amorphous transition metal-metalloid alloys has been investigated extensively in the past [1]. Most of them were prepared by rapid quenching of the melt, which usually works well at eutectic compositions. In the present paper we investigate the chemical and topological short range order of amorphous titanium-silicides, which can be prepared by sputtering within a wide range of composition from 40 up to 87 atomic percent titanium.

The three partial pair correlation functions of a number of amorphous binaries have been determined by the isotopic substitution technique [1]. However, this method is only applicable in those cases where suitable stable isotopes are available, such as Ni-isotopes in Ni-based alloys. In the present work the partial pair correlation functions are determined from the combination of X-ray- and neutron diffraction experiments and a model calculation of the size effect function $G_{NC}(R)$. In order to obtain information on the three-dimensional structure of the amorphous alloys, atomic clusters are produced by using the Reverse Monte Carlo (RMC) simulation method. Gaskell [2, 3] has proposed trigonal prisms as a structural unit for amorphous transition metal-metalloid alloys. In each unit a central metalloid atom is surrounded by six transition metal atoms forming a trigonal prism with three further metalloid atoms on the square faces of the prism. These trigonal prisms are frequently found in crystalline phases like Fe_3C, Fe_3P, and Ti_3Si. Therefore the amorphous clusters of the titanium-silicides were investigated concerning the existence of trigonal prisms using the method as introduced by Lamparter [4].

* Laboratoire Leon Brillouin, Laboratoire Commun CEA-CNRS, 91191 Gif-sur-Yvette, Cedex, France.

Reprint requests to Prof. Dr. S. Steeb.

2. Theoretical Fundamentals

In the following a summary of the relations used in the present work to describe the structure of binary amorphous alloys is given. For a detailed presentation see e.g. [1].

2.1 Faber-Ziman Formalism

The total structure factor $S^{FZ}(Q)$ according to the Faber-Ziman definition [5] is obtained from the coherently scattered intensity per atom I_{coh}:

$$S^{FZ}(Q) = \frac{I_{coh}(Q) - [\langle b^2\rangle - \langle b\rangle^2]}{\langle b\rangle^2}, \tag{1}$$

where $Q = (4\pi/\lambda)\sin\Theta$, 2Θ is the scattering angle, λ is the wavelength of the radiation, $\langle b\rangle = c_A b_A + c_B b_B$, $\langle b^2\rangle = c_A b_A^2 + c_B b_B^2$, c_A, c_B are the atomic concentrations of the components A and B, and b_A, b_B are the mean coherent scattering lengths (which depend on Q in the case of X-rays). The total structure factor is a weighted sum of the partial structure factors $S_{ij}^{FZ}(Q)$:

$$S^{FZ}(Q) = \frac{c_A^2 b_A^2}{\langle b\rangle^2} S_{AA}^{FZ}(Q) + \frac{c_B^2 b_B^2}{\langle b\rangle^2} S_{BB}^{FZ}(Q) + \frac{2 c_A c_B b_A b_B}{\langle b\rangle^2} S_{AB}^{FZ}(Q). \tag{2}$$

0932-0784 / 95 / 0800-0749 $ 06.00 © – Verlag der Zeitschrift für Naturforschung, D-72027 Tübingen

Dieses Werk wurde im Jahr 2013 vom Verlag Zeitschrift für Naturforschung in Zusammenarbeit mit der Max-Planck-Gesellschaft zur Förderung der Wissenschaften e.V. digitalisiert und unter folgender Lizenz veröffentlicht: Creative Commons Namensnennung-Keine Bearbeitung 3.0 Deutschland Lizenz.

This work has been digitalized and published in 2013 by Verlag Zeitschrift für Naturforschung in cooperation with the Max Planck Society for the Advancement of Science under a Creative Commons Attribution-NoDerivs 3.0 Germany License.

Zum 01.01.2015 ist eine Anpassung der Lizenzbedingungen (Entfall der Creative Commons Lizenzbedingung „Keine Bearbeitung") beabsichtigt, um eine Nachnutzung auch im Rahmen zukünftiger wissenschaftlicher Nutzungsformen zu ermöglichen.

On 01.01.2015 it is planned to change the License Conditions (the removal of the Creative Commons License condition "no derivative works"). This is to allow reuse in the area of future scientific usage.

The partial pair correlation functions $G_{ij}^{FZ}(R)$ are obtained from the $S_{ij}^{FZ}(Q)$ by Fourier transformation:

$$G_{ij}^{FZ}(R) = \frac{2}{\pi} \int_0^\infty Q\,[S_{ij}^{FZ}(Q) - 1] \sin(Q\,R)\,dQ, \quad (3)$$

where R is the atomic distance.

$G_{ij}^{FZ}(R)$ is related to the partial atomic density function of j-type atoms around an i-type atom, $\varrho_{ij}(R)$, by

$$G_{ij}^{FZ}(R) = 4\pi R[\varrho_{ij}(R)/c_j - \varrho_0], \quad (4)$$

where ϱ_0 is the mean atomic density. The partial coordination number Z_{ij} can be determined by integration:

$$Z_{ij} = \int_{R_1}^{R_2} 4\pi R^2 \varrho_{ij}(R)\,dR.$$

2.2 Bhatia-Thornton formalism

With the Bhatia and Thornton formalism [6] the total structure factor

$$S^{BT}(Q) = \frac{I_{coh}(Q)}{\langle b^2 \rangle} \quad (5)$$

is subdivided into three weighted partial structure factors $S_{NN}(Q)$, $S_{NC}(Q)$, and $S_{CC}(Q)$:

$$S^{BT}(Q) = \frac{\langle b \rangle^2}{\langle b^2 \rangle} S_{NN}(Q) + \frac{c_A c_B (b_A - b_B)^2}{\langle b^2 \rangle} \cdot S_{CC}(Q) + 2\frac{\langle b \rangle (b_A - b_B)}{\langle b^2 \rangle} S_{NC}(Q), \quad (6)$$

where $S_{NN}(Q)$ is the partial structure factor of the density-density correlations, $S_{CC}(Q)$ is the partial structure factor of the concentration-concentration correlations, and $S_{NC}(Q)$ is the partial structure factor of the density-concentration correlations. The correlation functions $G_{CC}(R)$, $G_{NN}(R)$, and $G_{NC}(R)$ are obtained from the partial structure factors $S_{CC}(Q)$, $S_{NN}(Q)$, and $S_{NC}(Q)$ by Fourier transformation. The Faber-Ziman formalism and the Bhatia-Thornton formalism are interrelated by the relations

$$G_{NN}(Q) = c_A^2 G_{AA}^{FZ}(R) + c_B^2 G_{BB}^{FZ}(R) + 2\,c_A c_B G_{AB}^{FZ}(R), \quad (7)$$

$$G_{CC}(Q) = c_A c_B (G_{AA}^{FZ}(R) + G_{BB}^{FZ}(R) - 2\,G_{AB}^{FZ}(R)), \quad (8)$$

$$G_{NC}(Q) = c_A c_B [c_A (G_{AA}^{FZ}(R) - G_{AB}^{FZ}(R)) - c_B (G_{BB}^{FZ}(R) - G_{AB}^{FZ}(R))]. \quad (9)$$

3. Experimental and Data Reduction

3.1 Specimen Preparation

Platelets of amorphous $Ti_{100-x}Si_x$ ($13 \leq x \leq 60$) were produced by sputtering. Aluminium foil was used as substrate which was dissolved by a caustic soda solution after the sputtering process. For the details we refer to [7].

3.2 X-ray Diffraction

The X-ray diffraction experiments were done on a diffractometer (Siemens; D500) in transmission mode. Using Mo–K_α radiation, the Q-range was $0.8\,\text{Å}^{-1} \leq Q \leq 14.6\,\text{Å}^{-1}$. The measured intensities were corrected for Compton scattering [8, 9], polarisation [10], and absorption [9, 10]. The conversion into absolute scattering units was done according to Krogh-Moe [11]. Figure 1 shows the total structure factors $S^{FZ}(Q)$ as obtained with X-rays.

3.3 Neutron Diffraction

The neutron diffraction experiments were performed at LLB-Saclay with the 7C2 goniometer. Using $\lambda = 0.7$ Å, the Q range from $0.34\,\text{Å}^{-1}$ up to $16.0\,\text{Å}^{-1}$ was covered by the multicounter. The measured intensities were corrected for background and absorption according to Paalman and Pings [12], multiple scattering according to Sears [13], and inelastic scattering according to Placzek [14]. The conversion into absolute scattering units was done according to Krogh-Moe [11]. The corrected intensity curve of amorphous $Ti_{75}Si_{25}$ is shown as dashed line in Figure 2. It exhibits a strong decrease with increasing Q.

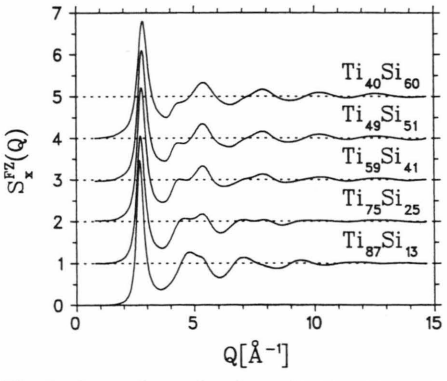

Fig. 1. Amorphous titanium-silicides; X-ray diffraction: total structure factors $S_x^{FZ}(Q)$.

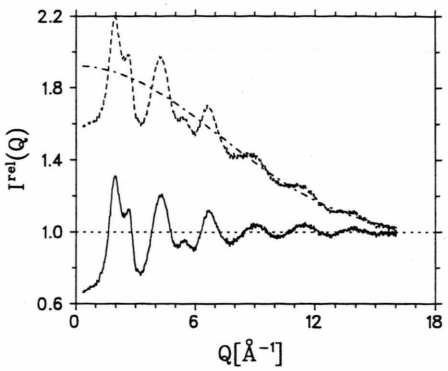

Fig. 2. Amorphous $Ti_{75}Si_{25}$; neutron diffraction: correction for the incoherent scattering contribution of hydrogen; – – – intensity corrected for background and absorption; –·–·– incoherent scattering contribution of hydrogen; —— intensity corrected for background, absorption, and incoherent scattering of hydrogen.

The reason for this behaviour is the incoherent scattering from a hydrogen contamination in the specimen of about 3 pct. The separation of this scattering contribution was done by the so called Fourier filtering method: In the Fourier transform of the intensity the hydrogen contribution occurs as a peak at R-values well below the atomic distances. This peak alone is transformed back into Q-space and thus yields the intensity contribution of hydrogen (–·–·– in Figure 2). The full line in Fig. 2 represents the intensity corrected for background and absorption, as well as for incoherent hydrogen scattering.

Furthermore, the contribution of hydrogen to the multiple scattering had to be taken into account. Figure 3 shows the total structure factors $S^{FZ}(Q)$ of the amorphous titanium-silicides, as obtained with neutrons.

4. Determination of the Partial Structure Factors and the Partial Pair Correlation Functions of $Ti_{87}Si_{13}$ by Neglecting the Si–Si Correlation

The total structure factors $S_{x,n}^{FZ}$ of $Ti_{87}Si_{13}$ which have been obtained by X-ray- and neutron diffraction are composed of the partial structure factors S_{ij}^{FZ} according to (2) as

$$S_x^{FZ}(Q) = 0.834\, S_{TiTi}^{FZ}(Q) + 0.008\, S_{SiSi}^{FZ}(Q) + 0.158\, S_{TiSi}^{FZ}(Q), \quad (10)$$

$$S_n^{FZ}(Q) = 1.488\, S_{TiTi}^{FZ}(Q) + 0.048\, S_{SiSi}^{FZ}(Q) - 0.536\, S_{TiSi}^{FZ}(Q). \quad (11)$$

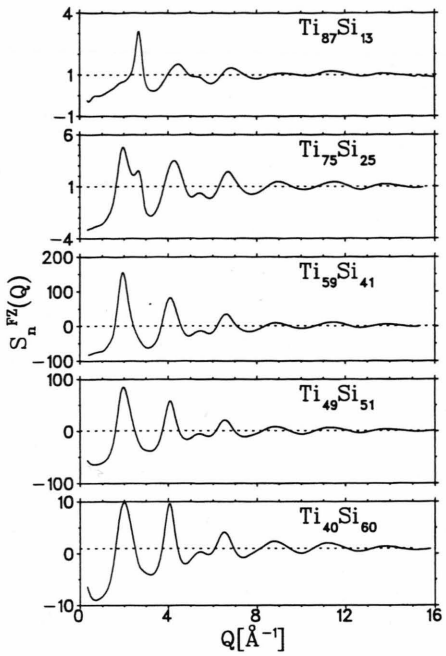

Fig. 3. Amorphous titanium-silicides; neutron diffraction: total structure factor $S_n^{FZ}(Q)$.

Table 1. Amorphous $Ti_{87}Si_{13}$ and amorphous $Ti_{84}Si_{16}$ [15]; atomic distances R_{ij}, partial coordination numbers Z_{ij}, widths of pair distribution w_{ij} and chemical short range order parameters η_{ij}.

	R_{TiTi}[Å]	R_{TiSi}[Å]	Z_{TiTi}	Z_{TiSi}	Z_{SiTi}	w_{TiTi}	w_{TiSi}	η_{TiSi}
$Ti_{87}Si_{13}$	2.87	2.67	12.2	1.5	10.0	0.43	0.45	0.11
$Ti_{84}Si_{16}$	2.90	2.64	11.5	1.8	9.4	0.45	0.33	0.14

The weighting factors in (10) are given for $Q=0$. The weighting factor of the Si–Si correlation is very small in the X-ray and in the neutron experiment. Thus the partial structure factors $S_{TiTi}^{FZ}(Q)$ and $S_{TiSi}^{FZ}(Q)$ can be determined by neglecting the Si–Si correlation. The result is shown in Figure 4a. The Fourier transforms $G_{TiTi}^{FZ}(R)$ and $G_{TiSi}^{FZ}(R)$ are shown in Fig. 4b, and the structural parameters are listed in Table 1 together with the corresponding values for amorphous $Ti_{84}Si_{16}$ which were reported in [15]. The atomic distances R_{ij} were taken from the position of the first peak of the $G_{ij}^{FZ}(R)$ functions. The partial coordination numbers Z_{ij} were obtained by applying the Gauss fitting method to the peaks of the $\varrho_{ij}(R)$ functions. The widths w_{ij} of the pair distributions were taken from the first peaks of $G_{ij}^{FZ}(R)$. The chemical short range

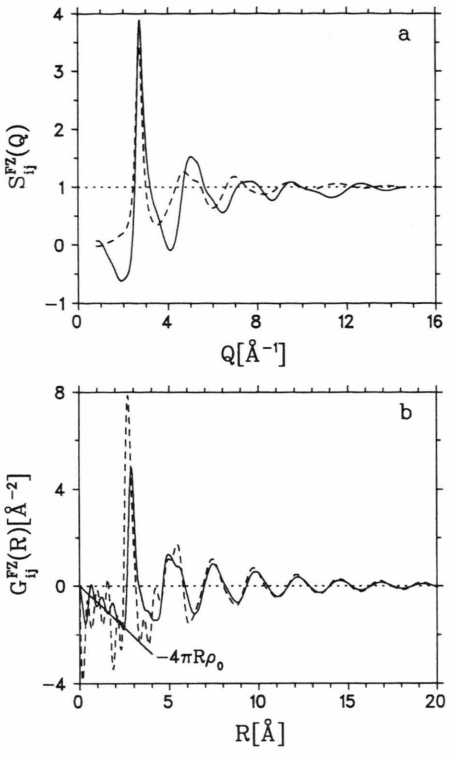

Fig. 4. Amorphous $Ti_{87}Si_{13}$: a) Faber-Ziman partial structure factors; b) partial pair correlation functions; —— TiTi, --- Ti–Si.

order parameters η_{ij} were calculated according to Cargill and Spaepen [16]. $G_{TiTi}^{FZ}(R)$ and $G_{TiSi}^{FZ}(R)$ show a sharp first maximum. The first peak of $G_{TiSi}^{FZ}(R)$ is well separated from the following maxima by a minimum, where $G_{TiSi}^{FZ}(R)$ drops down to the $-4\pi R\varrho_0$ line, i.e. where $\varrho_{TiSi}(R)=0$. This well defined Ti–Si coordination shell reflects the chemical bonding between the metal atoms and the metalloid atoms which dominates the chemical short range order (CSRO). The width of the first peak in the Ti–Si pair distribution is smaller for $Ti_{84}Si_{16}$ than for $Ti_{87}Si_{13}$. Apparently the Ti–Si correlation is sensitive to small changes of the Si-content when the Si-concentration of the alloys is small. The width of the pair distribution of the Ti–Ti correlation has comparable values for both samples.

The comparison of the atomic distances R_{TiTi} in Table 1 with the Goldschmidt diameter of Ti(D_{TiTi}^{G} = 2.91 Å) [17] shows a good agreement for $Ti_{84}Si_{16}$, whereas the atomic distance R_{TiTi} for $Ti_{87}Si_{13}$ is slightly smaller. The experimental atomic distance R_{TiSi} in Table 1 shows also a good agreement with a calculated atomic distance $R_{TiSi}^{c}=2.63$ Å for $Ti_{84}Si_{16}$, using the Goldschmidt diameters of Ti and Si ($D_{SiSi}^{G}=2.34$ Å). For $Ti_{87}Si_{13}$ the experimental atomic distance R_{TiSi} is slightly larger than the calculated atomic distance R_{TiSi}^{c}. The chemical short range order parameters η_{TiSi} in Table 1 are comparable, indicating a preference for compound formation in both titanium-silicides. The chemical short range order parameters of other metal-metalloid glasses such as $Ni_{81}B_{19}$ and $Ni_{80}P_{20}$ have similar values ($\eta_{NiB}=0.17$ [18], $\eta_{NiP}=0.13$ [19]).

5. Determination of the Partial Pair Correlation Functions for the Amorphous Titanium-Silicides

The method described in Chapt. 4 can only be applied for small Si concentrations, where the contribution of the Si–Si correlation can be neglected.

In the following a method is described to evaluate the partial pair correlation functions from a set of two diffraction experiments, with X-rays and neutrons in the present case, and a third body of structural information from a model calculation. For setting up a model two conditions are essential:

i) As a third body of structural information, to be simulated by a model, a suitable one should be chosen which is expected to be insensitive to the degree of the CSRO.

ii) The information about the structure, already known from the experimental data, should be implemented into the model.

The size effect function $G_{NC}(R)$ is most suitable to meet these conditions, because it is mainly determined by the atomic diameters of the constituents in the alloy.

In some previous combined X-ray and neutron diffraction investigations the size effect was neglected by setting the Bhatia-Thornton partial correlation function $G_{NC}(R)=0$ (see e.g. [20]). Because the diameters of the constituents in metallic glasses usually are quite different, in some investigations the $G_{NC}(R)$ function was calculated using the Percus-Yevick hard-sphere model [21] which, however, does not account for chemical interactions. In the present paper $G_{NC}(R)$ was calculated using a cluster relaxation algorithm given in [22]. The pair potentials were chosen in such a way as to obtain best agreement between the simu-

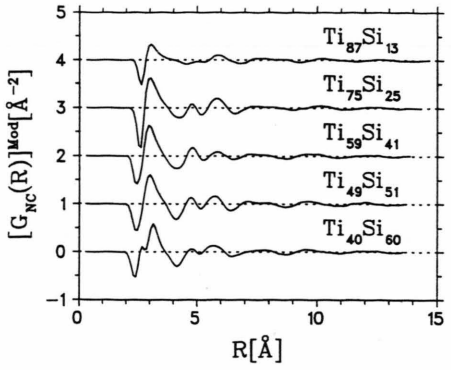

Fig. 5. Size effect function for amorphous titanium-silicides from cluster relaxation model.

Table 2. Amorphous titanium-silicides; atomic distances R_{ij}, partial coordination numbers Z_{ij}, chemical short range order parameters η_{ij} and normalized chemical short range order parameters η^0_{ij}.

	R_{TiTi} [Å]	R_{TiSi} [Å]	R_{SiSi} [Å]	Z_{TiTi}	Z_{TiSi}	Z_{SiTi}	Z_{SiSi}	η_{TiSi}	η^0_{TiSi} [%]
$Ti_{87}Si_{13}$	2.86	2.68	–	12.2	1.5	10.0	–	0.11	100
$Ti_{75}Si_{25}$	2.91	2.62	–	11.0	2.9	8.7	–	0.21	100
$Ti_{59}Si_{41}$	2.96	2.62	2.36	9.0	4.9	7.1	1.2	0.20	48
$Ti_{49}Si_{51}$	3.02	2.62	2.46	7.6	5.9	5.7	2.4	0.14	23
$Ti_{40}Si_{60}$	3.14	2.64	2.48	6.6	6.8	4.5	3.6	0.07	7

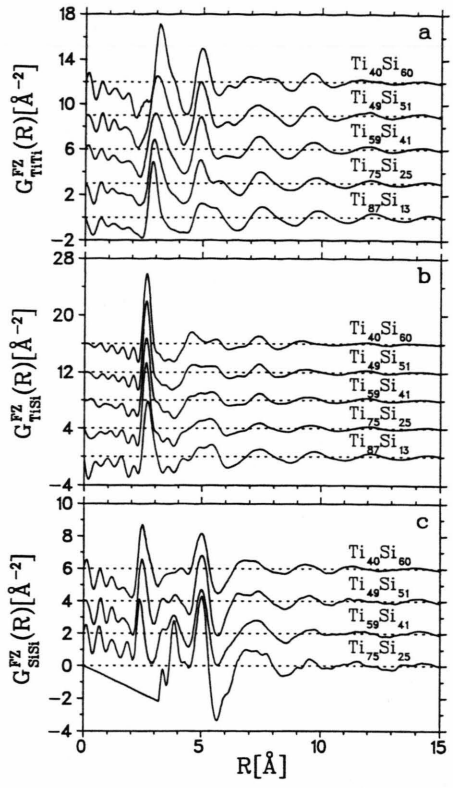

Fig. 6. Amorphous titanium-silicides: partial pair correlation functions; a) $G^{FZ}_{TiTi}(R)$; b) $G^{FZ}_{TiSi}(R)$; c) $G^{FZ}_{SiSi}(R)$.

lated and the experimental total $G^{FZ}_x(R)$ and $G^{FZ}_n(R)$ functions (for the details see [7]). The CSRO was incorporated by a stronger interaction potential for Ti–Si pairs than for Ti–Ti and Si–Si pairs. Figure 5 shows the Bhatia-Thornton correlation function $[G_{NC}(R)]^{Mod}$ obtained from the model.

From the X-ray and neutron diffraction results, combined with the calculated $G_{NC}(R)$ functions, the partial $G^{FZ}_{TiTi}(R)$, $G^{FZ}_{TiSi}(R)$, and $G^{FZ}_{SiSi}(R)$ functions were calculated and plotted in Figure 6a–c. Table 2 shows the atomic distances R_{ij}, the partial coordination numbers Z_{ij}, the short range order parameters η_{TiSi} and the normalized short range order parameters η^0_{TiSi} for the amorphous titanium-silicides.

The partial correlation functions $G^{FZ}_{TiSi}(R)$ in Fig. 6b show a sharp first maximum with a width of 0.36 Å for $c_{Si} > 0.13$. The Ti–Si distance is fixed at 2.62 Å, although the Ti–Ti and the Si–Si distances increase with increasing Si concentration. This indicates that the short range order is governed by the chemical bonding between the metal atoms and the metalloid atoms. Only the Ti-rich alloy $Ti_{87}Si_{13}$ appears to have a disturbed chemical short range order since the Ti–Si distance is larger and the first peak of $G^{FZ}_{TiSi}(R)$ is not as sharp as for the other compositions.

On the other hand, the Ti–Ti correlation strongly depends on the composition since R_{TiTi} increases with increasing Si-content. The first peak of G^{FZ}_{TiTi} is broader than the first peak of G^{FZ}_{TiSi}. The partial pair correlation function $G^{FZ}_{SiSi}(R)$ can be determined for all concentrations except for $Ti_{87}Si_{13}$, where the contribution of the Si–Si correlation is very small for X-ray and neutron diffraction. It turned out that the physical oscillations of the $G^{FZ}_{SiSi}(R)$ function could not be discerned from the Fourier-ripples.

The same behaviour was observed for $Ti_{75}Si_{25}$ at R-values below 3.2 Å. In Fig. 6c this part of G^{FZ}_{SiSi} was replaced by the $-4\pi R\varrho_0$-line. Consequently, it is not possible to determine the nearest Si–Si distance in amorphous $Ti_{75}Si_{25}$.

The partial coordination numbers Z_{ij} show the expected dependence on the composition. Z_{TiTi} and Z_{SiTi} decrease and Z_{TiSi} as well as Z_{SiSi} increases with increasing Si-content. It is important to note that the decrease of Z_{SiTi} with increasing Si content does not support a previous suggestion [23] that in amorphous transition metal-metalloid alloys the configuration of 9 metal atoms around a metalloid atom is formed as a rather stable one, independently of the composition.

The short range order parameter η_{TiSi} according to Cargill and Spaepen is positive, which means that all investigated alloys prefer compound formation. The short range order parameters for $Ti_{87}Si_{13}$ and $Ti_{75}Si_{25}$ were calculated by neglecting the Si–Si correlation, which has the consequence that the normalized short range order parameter η^0_{TiSi} attains 100%. A realistic value for η^0_{TiSi} cannot be given without knowing Z_{SiSi}. For the other samples the values of η^0_{TiSi} indicate that the compound formation tendency decreases with increasing Si-content.

6. Creation of Atomic Clusters by Reverse Monte Carlo Simulation (RMC)

The partial pair correlation functions represent a one-dimensional description of the three-dimensional structure of an amorphous alloy. Using the RMC method according to McGreevy and Pusztai [24], a three-dimensional cluster can be obtained which is consistent with the experimental pair correlation functions.

As a starting configuration for the RMC run, in each case the cluster of 1500 atoms was taken, which has been created with the Brandt model, as described above. The refinement of the coordinations yielded optimum agreement between the calculated and the experimental $G^{\mathrm{FZ}}_{ij}(R)$ after about $5 \cdot 10^5$ accepted atomic displacements. For $Ti_{87}Si_{13}$ the total pair correlation functions were used because the partial pair correlation function $G^{\mathrm{FZ}}_{\mathrm{SiSi}}(R)$ could not be determined. Figure 7 shows for amorphous $Ti_{75}Si_{25}$ as an example the perfect agreement between the calculated and experimental partial pair correlation functions. The agreement with the other amorphous Ti–Si alloys is comparable [7].

7. Analysis of the Atomic Cluster of $Ti_{75}Si_{25}$ as Created by the RMC-Method

Figure 8 shows the histogram of the number of Ti-neighbours around Si obtained from the RMC cluster of the alloy $Ti_{75}Si_{25}$. As the upper limit of the Ti–Si distance the minimum position of $G^{\mathrm{FZ}}_{\mathrm{TiSi}}(R)$ at $R = 3.34$ Å was used. The most frequent coordination number, $Z_{\mathrm{SiTi}} = 9$, is the same as for a face capped trigonal prism, and it is the same as for crystalline Ti_3Si.

The phase diagram for the titanium-silicon system exhibits a number of crystalline phases. In [7] a detailed comparison was carried out between the partial pair distributions of the amorphous Ti–Si alloys and the distance distributions in the crystalline Ti–Si

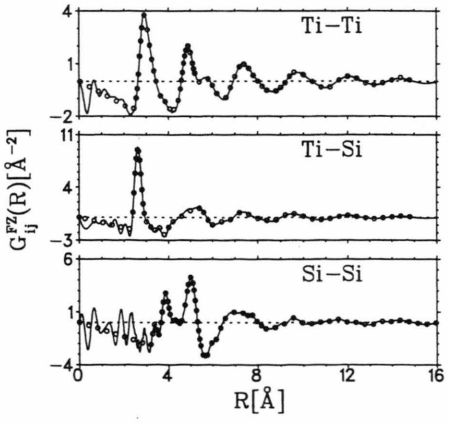

Fig. 7. Amorphous $Ti_{75}Si_{25}$: partial pair correlation functions; — $G^{\mathrm{FZ}}_{ij}(R)$ using X-ray diffraction, neutron diffraction and $G_{\mathrm{NC}}(R)$ from Fig. 5, ooo RMC-calculations.

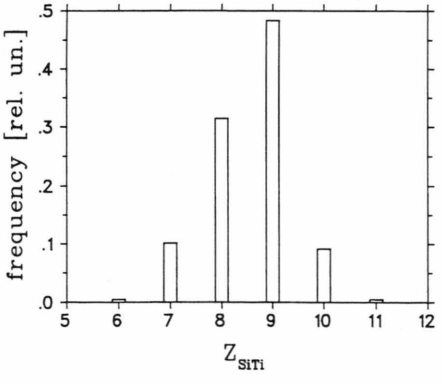

Fig. 8. Amorphous $Ti_{75}Si_{25}$: histogram of Z_{SiTi} from RMC model.

phases and mixtures of them, respectively. The best agreement was found between the amorphous cluster of $Ti_{75}Si_{25}$ and the crystalline phase Ti_3Si, which is mainly built up from trigonal Ti-prisms centered by Si- and capped by further Ti-atoms [25, 26]. This is the reason why the RMC clusters were analyzed in terms of trigonal prismatic arrangements according to the methods as introduced in [4]. Of course, within the amorphous cluster as produced by the RMC-method the trigonal prisms are expected to be distorted. A trigonal prism can be represented by two tetrahedra with a Si-atom as common vertex, as sketched in the inset of Figure 9 b. The two tetrahedra can be tilted and rotated compared to the ideal prism. The quality of the trigonal prismatic arrangement can be described by a tilting angle α and an angle β of rotation between the upper 3 Ti-atoms and the lower 3 Ti-atoms.

During the analysis of the RMC clusters in terms of such configurations a double tetrahedron was accepted within the following limits: 1) The 6 Ti-atoms are nearest neighbours of the central Si-atom, and the 3 Ti-atoms in each tetrahedron are mutual nearest neighbours, where the outer limit of the coordination shell is given by the first minimum in the corresponding pair correlation function. 2) The tilting angle α is within the range $0 \leq \alpha \leq 15°$. The histograms of the rotation angle $|\beta| \leq 60°$ were recorded for the different values of Z_{SiTi}.

Figure 9 a shows for amorphous $Ti_{75}Si_{25}$ the frequency of the angle of rotation β for $Z_{SiTi}=8$, 9, and 10, respectively. Those configurations where β is small may be classified as more or less distorted trigonal prisms. Apparently, for $Z_{SiTi}=9$ the tendency to form trigonal prismatic arrangements is most pronounced, whereas for $Z_{SiTi}=10$ no preference for trigonal prisms is observed.

The result for the $Ti_{75}Si_{25}$ cluster as shown in Fig. 9 a and the $Ti_{87}Si_{13}$ cluster as shown in [7] is, that for Si-atoms which are surrounded by 9 Ti-atoms there is a tendency to form trigonal prisms. In the atomic clusters of amorphous $Ti_{59}Si_{41}$, $Ti_{49}Si_{51}$, and $Ti_{40}Si_{60}$ no accumulation at an angle of rotation of 0° has been found [7], and thus these amorphous alloys have no preference of trigonal prismatic arrangements. Noting that within the amorphous cluster for $Ti_{59}Si_{41}$ only 0.2% of the Si-atoms and in the clusters of $Ti_{49}Si_{51}$ and $Ti_{40}Si_{60}$ no Si-atoms at all are surrounded by 9 Ti-atoms [7], it is suggested that the preferred occurrence of trigonal prisms is associated

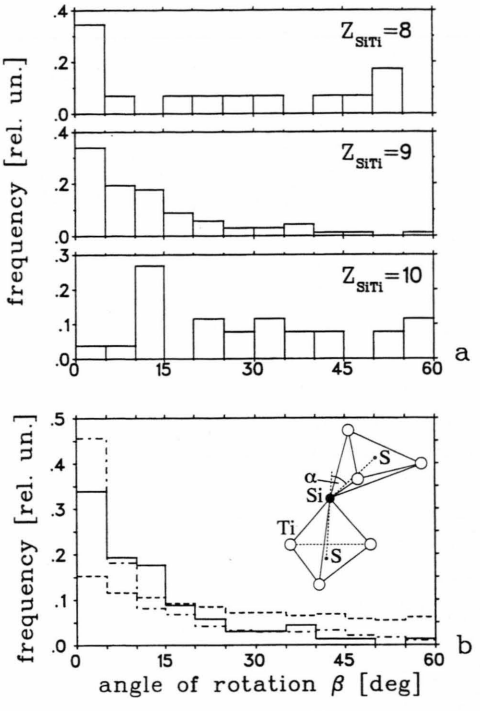

Fig. 9. Amorphous $Ti_{75}Si_{25}$: a) histogram of β for three coordination numbers Z_{SiTi}. b) histogram of β for $Z_{SiTi}=9$; —— amorphous $Ti_{75}Si_{25}$ (RMC model); – – – statistical reference cluster RC 1; –·– reference cluster RC 2. α is the tilting angle between the two Ti-tetrahedra sketched in b).

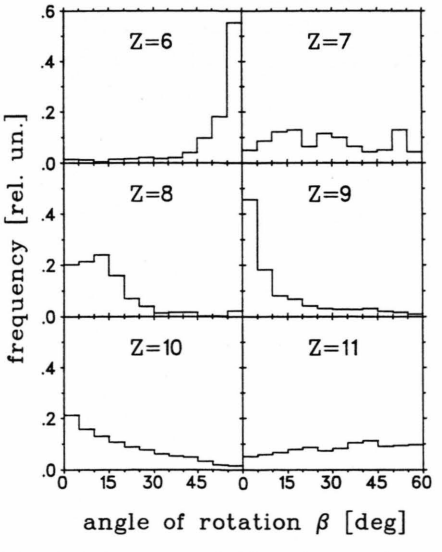

Fig. 10. Histograms of β for reference clusters RC 2 for different Z_{SiTi}.

with the coordination number 9, although a prism consists of only 6 atoms.

In the following the question is addressed whether the preference of trigonal prismatic arrangements at the coordination number $Z_{SiTi}=9$ is a geometrical effect or a stereochemical effect. This question can be investigated by constructing reference clusters where only the size effect is incorporated. According to the method described in [4], two types of statistical reference clusters were constructed. In the first type (RC1) Z_{SiTi} Ti-atoms were distributed randomly around a central Si-atom at a distance taken as the experimental Ti–Si distance R_{TiSi} with the constraint that the smallest distance between two Ti-atoms corresponds to the smallest R-value of $G_{TiTi}(R)$. In the second type of reference clusters (RC2) the Ti-atoms, after their positioning, were moved in a random way until the average of their mutual distances became as large as possible, i.e. until their distribution on the sphere with radius R_{TiSi} became most uniform. The reference clusters RC1 and RC2 were analyzed in the same way as the amorphous cluster of $Ti_{75}Si_{25}$. The result for the coordination number $Z_{SiTi}=9$ is shown in Fig. 9 b together with the result from the RMC cluster from Figure 4 a. We state that the tendency to form trigonal prisms is stronger for the RMC cluster than for the statistical reference cluster RC1, but it is weaker than for the reference cluster RC2.

Figure 10 shows the histograms of the rotation angle β for the reference clusters RC2 with different coordination numbers $6 \leq Z_{SiTi} \leq 11$. It reveals that prismatic packing is most preferred in case of the coordination number $Z_{SiTi}=9$, which means that this preference can be explained in a quite simple way as a geometrical effect.

From these observations we have to conclude that the preferred formation of trigonal prisms in amorphous $Ti_{75}Si_{25}$ with respect to a statistical distribution may be explained in two different ways: First, as a stereochemical effect, corresponding to that in the crystalline phase Ti_3Si, or secondly, as a geometrical effect, resulting from the tendency of 9 Ti neighbours to be distributed around Si with as large as possible mutual distances.

8. Conclusions

By X-ray diffraction, neutron diffraction and using a cluster relaxation model for the size effect the partial pair correlation functions of amorphous $Ti_{100-x}Si_x$ alloys ($13 \leq x \leq 60$) were determined. The partial pair correlation functions indicate a chemical bonding between the metal atoms and the metalloid atoms which dominates the chemical short range order. Three-dimensional atomic clusters were obtained using the Reverse Monte Carlo method. The amorphous atomic clusters were investigated for trigonal prismatic arrangements. The result is that trigonal prisms are preferred in that amorphous Ti–Si alloy ($Ti_{75}Si_{25}$) which has the same chemical composition as the corresponding crystalline phase (Ti_3Si). Comparison with hard sphere reference clusters shows that the preferred occurrence of trigonal prisms can be explained geometrically by a distribution of 9 Ti-neighbours around Si with the constraint that their mutual distances are as large as possible.

[1] P. Lamparter and S. Steeb, in: Material Science and Technology, Vol. 1, Chapt. 4, pp. 217–288. VCH Publishers Inc., Weinheim 1993.
[2] P. H. Gaskell, Nature London **289,** 474 (1981).
[3] P. H. Gaskell, in: H. Beck and H. J. Guentherodt, editors, Topics in Applied Physics, Vol. 53: Glassy Metals II, page 5, Springer Verlag, Berlin 1983.
[4] P. Lamparter, Proc. Euroconference '94 on Neutrons in Disordered Matter, Stockholm, 1994, Physica Scripta, to appear.
[5] T. E. Faber and J. M. Ziman, Phil. Mag. **11,** 153 (1965).
[6] A. Bhatia and D. E. Thornton, Phys. Rev. B **2,** 3004 (1970).
[7] A. Pojtinger, Doctor thesis, University of Stuttgart, 1994.
[8] J. H. Hubell et al., J. Phys. Chem. Ref. Data **4,** 2130 (1975).
[9] K. Sagel, Tabellen zur Röntgenstrukturanalyse, Springer-Verlag, Berlin 1950.
[10] C. N. J. Wagner, J. Non-Cryst. Sol. **31,** 1 (1978).
[11] J. Krogh-Moe, Acta Cryst. **9,** 951 (1956).
[12] H. H. Paalman and C. J. Pings, J. Appl. Phys. **33,** 2635 (1962).
[13] V. F. Sears, Adv. Phys. **24,** 1 (1975).
[14] G. Placzek, Phys. Rev. **31,** 377 (1952).
[15] P. Lamparter, A. Habenschuss, and A. H. Narten, J. Non-Cyst. Sol. **86,** 109 (1986).
[16] G. S. Cargill and F. Spaepen, J. Non-Cryst. Sol. **43,** 91 (1981).
[17] W. Hume Rothery and G. V. Raynor, The Structure of Metals and Alloys, 3rd Ed., Inst. of Metals, London 1954.
[18] P. Lamparter, W. Sperl, S. Steeb, and J. Blétry, Z. Naturforsch. **37 a,** 1223 (1982).
[19] P. Lamparter and S. Steeb, Proc. 5th Int. Conf. Rapidly Quenched Metals, Würzburg 1984, North-Holland, Amsterdam 1985, p. 459.

[20] G. Rainer-Harbach, P. Lamparter, F. Paasche, and S. Steeb, in T. Masumoto and K. Suzuki, editors, Proc. 4th Int. Conf. on Rapidly Quenched Metals RQIV, volume 1, page 315, Sendai, 1982, Japan Institute of Metals.
[21] N. W. Ashcroft and D. C. Langreth, Phys. Rev. **156,** 685 (1967).
[22] E. H. Brandt and H. Kronmüller, J. Phys. F **17,** 1291 (1987).
[23] P. Lamparter, in: Atomic Transport and Defects in Metals by Neutron Scattering, Springer Proc. in Phys. Vol. 10, Springer-Verlag, Berlin 1986, pp. 49–53.
[24] R. L. McGreevy and L. Pusztai, Mol. Simulation **1,** 359 (1988).
[25] W. B. Pearson, Handbook of Lattice Spacings and Structures of Metals and Alloys, Vol. 2, Pergamon Press, London 1967.
[26] W. Roßteutscher and K. Schubert, Z. Metalkde. **56,** 813 (1965).